Further Analysis of the Modulation of High Frequency Radar Spectra due to Sea-induced Antenna Platform Motion

[1,2]John Walsh, [1]Bernard Ryan, [1]Eric Gill, *Senior Member IEEE*, [3]Jacques El Khoury
[1]Faculty of Engineering and Applied Science, Memorial University of Newfoundland
[2]Northern Radar Inc., St. John's, Newfoundland, Canada
[3]SONDRA, Supélec, F-91192 Gif-sur-Yvette Cedex, France

***Abstract*—The scattering of high frequency electromagnetic waves from the ocean surface is considered for the case of the radiation source being a vertical pulsed antenna mounted on a floating platform while the receiving antenna is fixed on the shore. This represents a small extension to an earlier analysis by Walsh in which both the transmitting (TX) and receiving (RX) antennas were co-located on a floating platform and the effect of the sway was accounted for in the ocean cross section. It is known that additional features appear in the Doppler spectrum when the RX and TX antennas are permitted to sway slowly, and here a similar result is shown when only the TX antenna moves. It is seen in this case that the magnitude of the additional spectral features is reduced as compared to the case when both antennas are moving. As a motivation for continuing analytical work, a preliminary field result is depicted.**

I. Introduction

While the field of high frequency surface wave radar (HFSWR), in the context of ocean remote sensing, has considerably matured in the last three decades, there are still challenging questions, associated with the underlying science, that are worthy of continuing investigation. In more recent times, one of these, which has captured the interest of several HFSWR research teams, involves how to describe the modulation of the signals which results from the antenna(s) being mounted on a floating platform. Walsh [1] presented results, the analysis for which is partially found in [2] and is to appear in [3], describing the backscattered signal when the transmitter (TX) and receiver (RX) are co-located on a moving ocean platform.

More recently, El Khoury *et al.* [4] have reported on experimentation in which a signal transmitted from a landbased HFSWR was received by a monopole mounted on a tethered buoy – i.e, the fixed TX, moving RX situation. The spectra determined from that data show characteristics similar to the simulations conducted from Walsh's analysis [1] and [2].

In this paper, Walsh's analysis is revisited for the case when the TX antenna is moving and the RX antenna is fixed. While the concept is straightforward given the work that already exists in [1], [2], [3], the changes must be carefully propagated through the analysis. It will be shown that the first-order Bragg regions in this case contain similar extra peaks to those in the cited works. Those peaks extend into what is typically referred to as the second-order portions of the spectrum, but the energy contained in them differs from that observed when both TX and RX antennas are moving. Simulations may incorporate any appropriate sea spectrum but, for illustration purposes, a Pierson Moskowitz nondirectional spectrum [5] with a cardioid directional distribution is invoked here.

Section II of the paper summarizes the theory, and simulations are depicted and discussed in Section III where a preliminary field example is given. Section IV contains conclusions and a brief discussion of future directions to be pursued with respect to the problem of antenna motion.

II. Analytical Considerations

A. Electrical field for swaying, vertically polarized source with fixed receiver

The general bistatic geometry for a two-antenna system (one transmitter and one receiver) is depicted in Figure 1. The quantity $\delta\vec{\rho}_0$ is the small phasor change of the antenna separation, $\vec{\rho}$, and may be due to either or both antennas moving. Here, we wish to analyze the case in which the transmitter is mounted on a moving platform, say an ocean barge, while the RX antenna is on a fixed, nearby platform. In this case, we have essentially a monostatic geometry with $\rho = 0$, and the $\delta\vec{\rho}_0$ is associated only with the TX antenna. This case is depicted in Figure 2.

In keeping with [1], the motion vector $\delta\vec{\rho}_0$ is specified as

$$\delta\vec{\rho}_0 = a\sin(\omega_p t)\hat{\rho}_p \qquad (1)$$

where a is an amplitude depending on sea state, ω_p is the platform frequency, and $\hat{\rho}_p$ is the direction of $\delta\vec{\rho}_0$.

In [2], [3] the general form of the received electric field is given as

$$(E_{0_n}^{+})_1 \approx -jkC_0\frac{1}{(2\pi)^2}\int_{x_1}\int_{y_1}\hat{\rho}_1\cdot\vec{\nabla}_{x_1y_1}[\xi(x_1,y_1)] \cdot F(\rho_1)F(\rho_2)e^{jk\delta\vec{\rho}_0\cdot\hat{\rho}_1}\frac{e^{-jk(\rho_1+\rho_2)}}{\rho_1\rho_2}\,dx_1\,dy_1 \qquad (2)$$

Here, $C_0 = \dfrac{I\Delta\ell k^2}{j\omega\epsilon_0}$ is a constant for a dipole of length $\Delta\ell$ which carries a current I of radian frequency ω. The radiation wavenumber is k and a free-space permittivity of ϵ_0

978-1-4244-5222-4/10/$26.00 ©2010 IEEE

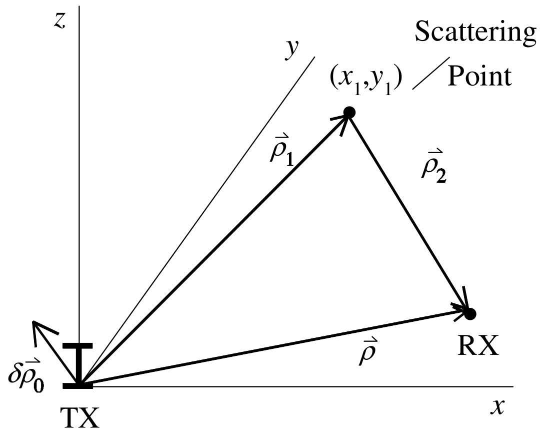

Fig. 1. Bistatic Radar Configuration

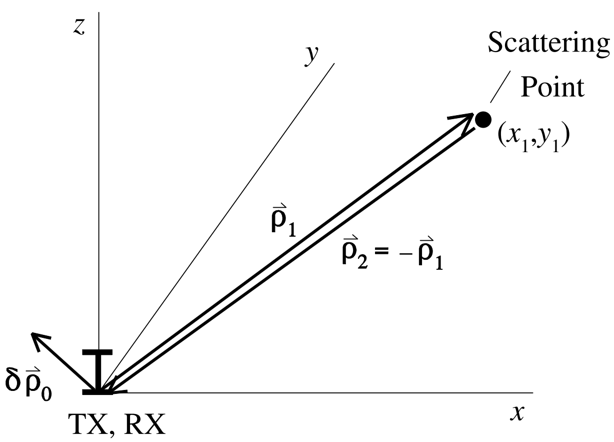

Fig. 2. First-order monostatic scattering geometry. The $\delta\vec{\rho}_0$ is associated with only the TX antenna here.

is used here. See Figures 1 and 2 for the distance parameters, ρ_1 and ρ_2 ($\hat{\rho}_1$ is the unit vector associated with $\vec{\rho}_1$) and ρ_2. The Fs are the Sommerfeld attenuation functions for a rough spherical earth and $\vec{\nabla}_{x_1y_1}[\xi(x_1,y_1)]$ is the gradient of the surface. Introducing a Fourier representation of the time-varying rough surface with random coefficients $P_{\vec{K}}$ associated with each surface wave vector $\vec{K}$, while allowing that only the TX antenna sways, it is possible to deduce after coordinate transformation that equation (2) becomes

$$
\begin{aligned}
(E_{0_n}^{+})_1 \quad \approx \quad & kC_0\frac{1}{(2\pi)^2}\sum_{\vec{K}} P_{\vec{K}} K \int_{\rho_1} \frac{F^2(\rho_1)}{\rho_1} e^{-j2k\rho_1} \\
& \cdot \int_0^{2\pi} \cos(\theta_1-\theta_K) e^{jk\delta\rho_0\cos(\theta_1-\theta_0)} \\
& \cdot e^{j\rho_1 K\cos(\theta_1-\theta_K)}\, d\theta_1\, d\rho_1 \qquad (3)
\end{aligned}
$$

where the angles θ_0, θ_1 and θ_K are associated with $\delta\vec{\rho}_0$, $\vec{\rho}_1$ and $\vec{K}$, respectively. Equation (3) differs from its counterpart in [2], [3] by having a $e^{jk\delta\rho_0\cos(\theta_1-\theta_0)}$ factor instead of a $e^{j2k\delta\rho_0\cos(\theta_1-\theta_0)}$ factor. The factor of 2 in the exponential of the earlier work is due to both the TX and RX antennas moving. Here, only the TX antenna moves.

B. A pulsed source and time-varying surface

In equation (3) the exact form of the current excitation and the surface coefficients for a time-varying surface have not yet been stipulated. Here we proceed as in [2], [3] and simply present the results. The current is now assumed to be a simple pulsed sinusoid for which k_0 $(= 2\pi/\lambda_0)$ is the representative wavenumber of the excitation and τ_0 is the pulse duration. The surface is taken to be represented as a zero-mean, stationary Gaussian process. Under these stipulations, an autocorrelation of the resulting time-domain electric field is carried out. The general form of this autocorrelation is simply

$$
R(\tau) = \frac{A_r}{2\eta_0}\langle (E_{0_n}^{+})_1(t+\tau)(E_{0_n}^{+})_1^{*}(t)\rangle \qquad (4)
$$

where $A_r = (\lambda_0^2/4\pi)G_r$ with G_r being the gain of the RX antenna, τ the interval between samples, and η_0 the intrinsic impedance of free space, while $*$ represents complex conjugation. After considerable, tedious algebra, Fourier transformation of the result and comparison with the standard radar range equation, it is deduced that the first-order ocean surface cross section, as a function of angular Doppler frequency ω_d, for the case of a swaying TX antenna and a fixed RX antenna is given by

$$
\begin{aligned}
\sigma(\omega_d) \;=\; & 2^3\pi k_0^2\Delta\rho \\
& \cdot \sum_{m=\pm 1}\int_K K^2 S(m\vec{K}) Sa^2\left[\frac{\Delta\rho}{2}(K-2k_0)\right] \\
& \cdot \left\{ J_0^2\left[\frac{aK}{2}\cos(\theta_K-\theta_{K_p})\right]\delta(\omega_d + m\sqrt{gK}) \right. \\
& + \sum_{n=1}^{\infty} J_n^2\left[\frac{aK}{2}\cos(\theta_K-\theta_{K_p})\right] \\
& \left[\delta(\omega_d + m\sqrt{gK} - n\omega_p) \right. \\
& \left.\left. +\; \delta(\omega_d + m\sqrt{gK} + n\omega_p)\right]\right\} dK\;. \qquad (5)
\end{aligned}
$$

In equation (5), $\Delta\rho$ is the scattering patch width (this equals $c\tau_0/2$, with c being the free space speed of light), $S(\vec{K})$ is the ocean spectrum as a function of wave vector $\vec{K}$ $(\equiv (K,\theta_K))$, $Sa(x) = \sin(x)/x$, and the J_n are Bessel functions of order n, while δ is the Dirac delta function. Also, $\theta_{K_p} = \omega_p^2/g$, g being the gravitational acceleration, and θ_{K_p} is the direction of $\vec{K}_p$, the dominant ocean wave vector assumed to be responsible for the platform motion.

Equation (5) consists of an infinite number of Bessel functions. When simulating the cross section, this equation will have to be approximated using a finite number of terms. It is therefore useful to decompose the equation for different values of n. In particular, for $n = 0$ equation (5) can be rewritten as

$$\begin{aligned}\sigma_0(\omega_d) \quad &= \quad 2^4 \pi k_0^2 \Delta\rho \frac{\sqrt{K} K^2}{\sqrt{g}} S a^2 \left[\frac{\Delta\rho}{2}(K - 2k_0)\right] \\ &\cdot J_0^2 \left[\frac{aK}{2}\cos(\theta_K - \theta_{K_p})\right] S[sgn(-\omega_d)\vec{K}] \quad (6)\end{aligned}$$

where the sifting property of the delta functions gives $K = \frac{\omega_d^2}{g}$. In view of the well-understood phenomenon of Bragg scattering, it is desirable to determine where σ_0 is maximum, as this corresponds to the first-order Bragg peaks. Clearly, this occurs when $K = 2k_0$ and therefore when $\omega_d = \sqrt{2gk_0}$. This result is consistent with the Bragg scattering condition for ground wave radars since $K = 2k_0$ implies $\lambda_K = \lambda_0/2$. In other words, the ocean wave wavelengths must be half the wavelength of the transmitted signal.

For higher values of n, equation (5) is best interpreted when split into two equations. These are

$$\begin{aligned}\sigma_{n1}(\omega_d) \quad &= \quad 2^4 \pi k_0^2 \Delta\rho \frac{\sqrt{K} K^2}{\sqrt{g}} S a^2 \left[\frac{\Delta\rho}{2}(K - 2k_0)\right] \\ &\cdot J_n^2 \left[\frac{aK}{2}\cos(\theta_K - \theta_{K_p})\right] S[sgn(-\omega_d + n\omega_p)\vec{K}] \quad (7) \\ &\text{with } K = \frac{(\omega_d - n\omega_p)^2}{g}\end{aligned}$$

and

$$\begin{aligned}\sigma_{n2}(\omega_d) \quad &= \quad 2^4 \pi k_0^2 \Delta\rho \frac{\sqrt{K} K^2}{\sqrt{g}} S a^2 \left[\frac{\Delta\rho}{2}(K - 2k_0)\right] \\ &\cdot J_n^2 \left[\frac{aK}{2}\cos(\theta_K - \theta_{K_p})\right] S[sgn(-\omega_d - n\omega_p)\vec{K}] \quad (8) \\ &\text{with } K = \frac{(\omega_d + n\omega_p)^2}{g}\end{aligned}$$

Again, these equations peak when $K = 2k_0$. However, from the sifting property of the delta functions, the peaks now occur when

$$\omega_d = \pm\sqrt{2gk_0} \pm n\omega_p. \quad (9)$$

These peaks are a result of the barge motion at the transmitter. From equation (9) it is clear that these peaks will be situated symmetrically with respect to the first-order Bragg peaks. It is important to note that if $\delta\vec{\rho}_0 = 0$ (i.e. if $a = 0$), equation (5) reduces to the cross section equation for monostatic operation where the both the transmitter and receiver are fixed – that is, the motion-induced peaks will not be present.

The difference between the cross section in equation (5) and that including the motion of both TX and RX antennas is a factor of 1/2 in the argument of the Bessel functions. The significance is discussed in the next section.

III. Depiction and Discussion of Cross Section

Initially, in Figure 3 we consider a comparison of the TX and RX antennas both fixed (TxFixed/RxFixed) with the case of the TX antenna moving but the RX antenna fixed (TxMoving/RxFixed). The wind speed is taken as 10 knots and the direction is perpendicular to the radar look direction. As noted in Section IIb, $\delta\vec{\rho}_0 = 0$ for the TxFixed/RxFixed case. From equation (5) this is observed to occur when $a = 0$. As a result the Bessel functions in equation reduce to $J_0(0) = 1$ and $J_n(0) = 0$ (for $n = 1, 2, 3...$). Consequently, the cross section will contain no peaks aside from the first-order peaks, which occur at the same Doppler frequency ($\omega_d = \sqrt{2gk_0}$) as in the TxMoving/RxFixed case. In both cases the large first-order peaks are nearly identical in magnitude and shape but when the TX antenna moves extra peaks appear and are depicted up to $n = 2$.

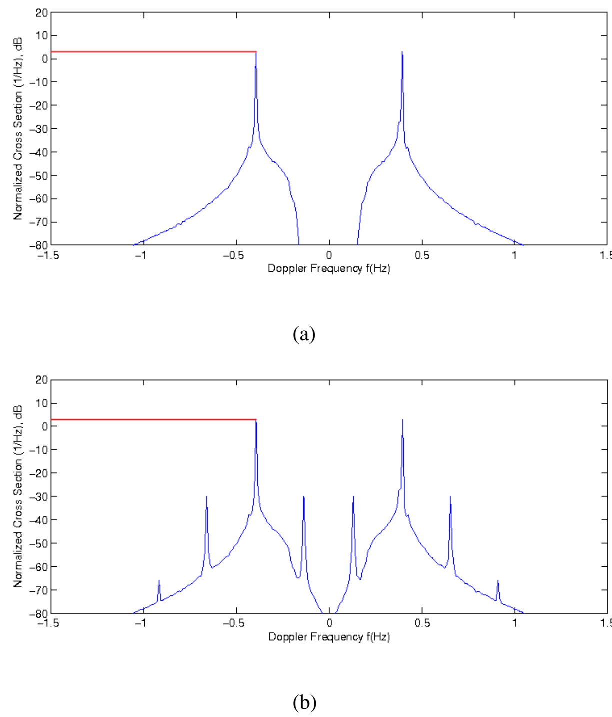

Fig. 3. Monostatic cross sections (a) TxFixed/RxFixed and (b) TxMoving/RxFixed.

In Figure 4, the case of both TX and RX antennas moving (TxMoving/RxMoving) is compared with the TxMoving/RxFixed case. In the latter instance, there is a reduction of several dBs in the secondary peaks caused by the motion. Nonetheless, these somewhat lower peaks, which overlap the second-order spectral regions, are still likely to have detrimental effects on the extraction of ocean wave information from HFSWR data. Fortunately, it seems that the same may not be true for current extraction as the usual first-order Bragg peaks are still clearly visible. The spectra here have been simulated for platform motion with sway frequency 0.261 Hz and an amplitude of 0.177 m. The operating frequency is 15 MHz and the wind speed is 10 knots for all cases. Figure 5 is an expanded view of the overlapped curves of Figure 4.

Finally, as a preliminary experimental example, we present in Figure 6 a spectrum obtained from using a fixed TX antenna and a buoy-mounted RX antenna. While this differs from

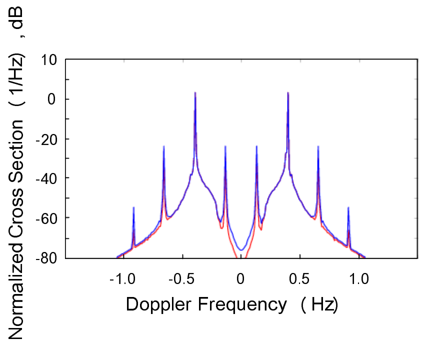

Fig. 4. Comparison of spectrum when both TX and RX are moving (blue) with that for TX moving and RX fixed (red).

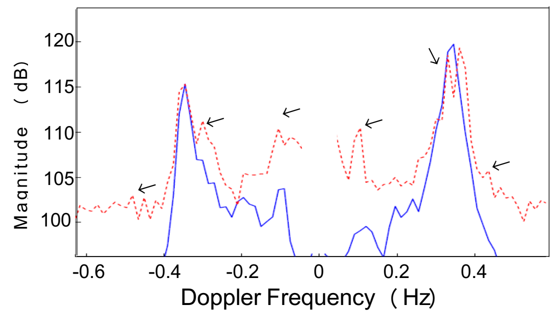

Fig. 6. Comparison of spectrum with both TX and RX fixed(blue) and that for TX fixed and RX moving (red) for field data obtained using a 12.38 MHz WERA radar system and a floating monopole. The arrows indicate motion-induced peaks.

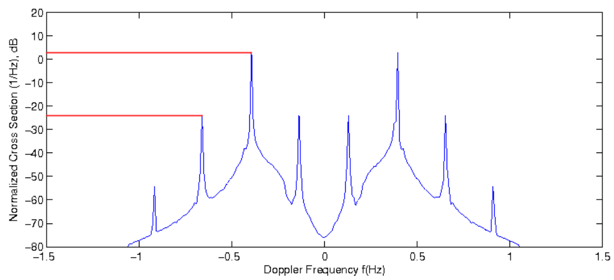

(a)

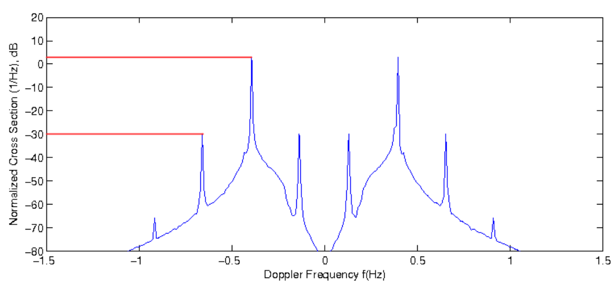

(b)

Fig. 5. Monostatic cross sections (a) TxMoving/RxMoving and (b) TxMoving/RxFixed.

the TxMoving/RxFixed case presented here, it still gives an indication of the extra energy spreading from the first order into the second order as a result of antenna motion. There is also evidence of extra spectral peaks in the case of the moving antenna. At this stage we have not attempted to reconcile the simulations of Figures 3–5 with the field data in Figure 6 in terms of ensuring corresponding parameters such as operating frequency and wind speeds and the magnitude and frequency of the antenna motion. In particular, it should be pointed out that the buoy-mounted antenna was close to shore and did not experience the same motion as assumed for the simulation. We simply present Figure 6 as evidence that the analytical result is worth further experimental investigation.

IV. Conclusions

Clearly, one of the benefits of mounting antennas on moving platforms is to extend coverage ranges for HFSWRs. As is shown here, however, this will mean having to cope with additional spectral features that may interfere with spectral inversion techniques presently used for surface parameter extraction. It is hoped that the ongoing theoretical analysis along with dedicated experimentation will provide further insight as to how to address these issues.

References

[1] J. Walsh, "The Effect of Barge Motion on HFSWR Ocean Clutter", Northern Radar Inc., St. John's, NL, 2004. (Contract Report Prepared for Raytheon Canada Limited, Waterloo, ON)

[2] J. Walsh, E. W. Gill, and W. Huang, "A Monostatic Ocean Scattering Cross Section for the Case of Surface Wave Radar Operating from a Floating Barge", *Proceedings, IEEE/MTS Oceans 2008*, Kobe, Japan, April 2008.

[3] J. Walsh, W. Huang, and E. W. Gill, "The First-order High Frequency Radar Ocean Surface Cross Section for an Antenna on a Floating Platform", *IEEE Trans. Ant. and Prop.*, under final review.

[4] J. El Khoury, R. Guinvarc'h, A. Bourges, and P. Flament, "An Experimentation of a Floating Antenna for HF Surface Wave Radar", *Radiowave Oceanography Workshop (ROW 2009)*, Split, Croatia, May 2009.

[5] Pierson, W., and L. Moskowitz, "A proposed spectral form for fully developed seas based upon the similarity theory of S.A. Kitaigorodskii", *J. Geophys. Res.*, vol. 69, pp. 5181–5190, 1964.